

Fat-Water Imaging: An Overview

Scott B. Reeder, MD, PhD

Departments of Radiology, Medical Physics, and Biomedical Engineering,
University of Wisconsin, Madison, WI

Chemical Shift Artifact

Magnetic resonance imaging (MRI) of protons in the human body exploits the fact that the relative magnetization of the proton is the highest of all nuclei, and more importantly, that the abundance of protons is extremely high – approximately 55 molar in pure water. Although a large percentage of protons are found in the form of water, with a single resonant peak at approximately 63.9 MHz at 1.5T, they are also found in large proportion, within the lipid component of adipose tissue. Fat has a complex spectrum with multiple peaks, the largest of which are shifted approximately 3.5ppm from the water peak, or about -210Hz from water at 1.5T (1). For the purposes of simplicity, we will assume that fat resonates at a single peak -210Hz from water.

MR reconstruction methods generally assume a single, sharp resonant peak for all structures within the body. Magnetic field gradients are then applied to create spatially dependent frequency shifts that are used facilitate the separation of the protons at different locations into an image. Typically, the Fourier transform is used decompose spins at different spatial locations. Unfortunately, the presence of fat creates a constant frequency shift, so that fat spins resonate approximately -210Hz more slowly than water. From the perspective of the Fourier transform, there is no difference between spins from fat, and those from water that are shifted spatially where the resonant frequency is -210 Hz lower, due to a lower magnetic field gradient. Figure 1 depicts a “one-dimensional” imaging experiment, with a small focus of water and fat located at the same position. In the presence of a readout gradient in the x -direction, the frequency of the spins increases across the image. The fat resonates more slowly than water, however, and after Fourier transformation (which ‘thinks’ there is only one species, water), the fat signal is mapped to a location closer to isocenter by an amount Δx . This “chemical shift” is directly related to frequency shift between water and fat and manifests as a shift of fat with respect to water in the readout direction of the image. No shift occurs in the phase encoding direction.

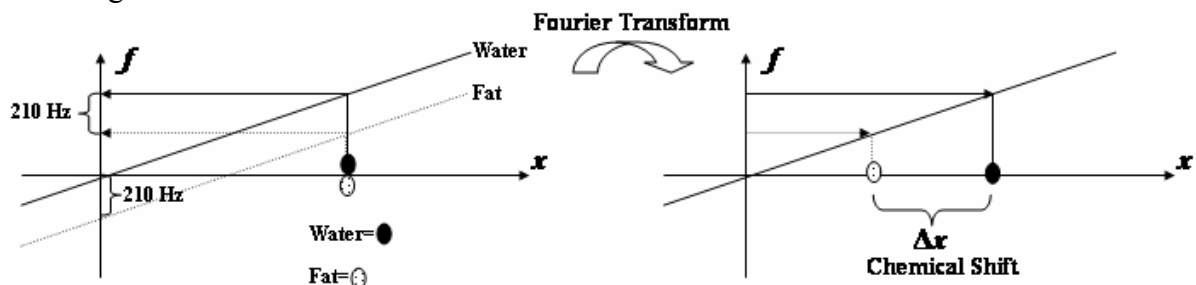


Figure 1: the signal from a small amount of water (solid oval) and fat (open oval) at the same x -position have different frequencies which are mapped to different spatial locations in the image, offset by Δx , after image reconstruction (Fourier transform).

Figure 2 shows an example of a T1W spin-echo image of a pelvic endometrioma (water signal) surrounded by fat. Fat is shifted in the readout direction creating “bunched up” signal on one aspect of the endometrioma and a rim of signal void on the opposite aspect.

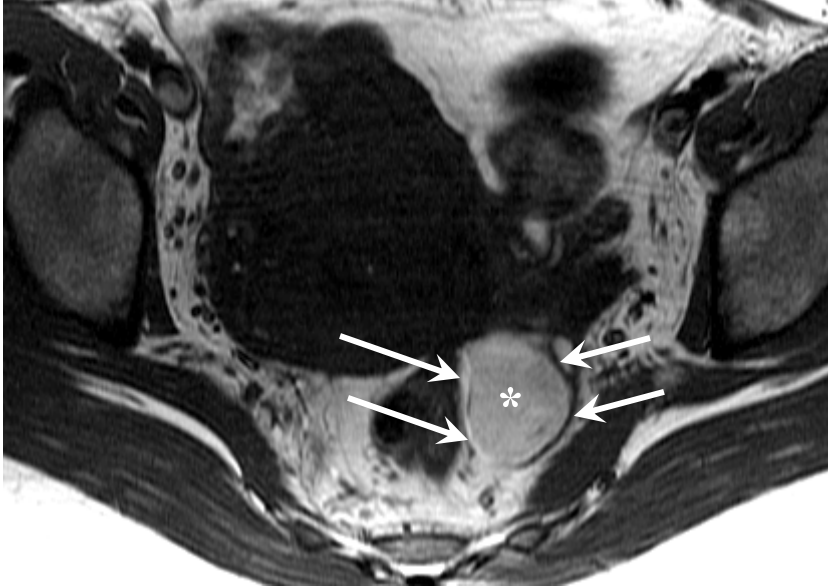


Figure 2: Axial T1W spin-echo image of an endometrioma (*) in the pelvis surrounded by fat. The fat is shifted in the readout direction (left-right), creating “bunched up” signal on the left aspect of the mass (left arrows) and a rim of signal void on the right aspect of the mass (right arrows).

The chemical shift artifact occurs only in the readout direction, and in this case the amount of chemical shift does little to degrade the image. In fact, this “artifact” helps distinguish this mass from a fatty masses such as a lipoma or ovarian dermoids.

As can be appreciated from figure 1, the slope of the readout gradient that is used will determine the actual shift in the image, Δx . The behavior of the readout gradient is determined by the choice of field of view, readout matrix size and the acquisition bandwidth. It can be shown that the chemical shift (in pixels) in the readout direction is,

$$\Delta x = \frac{N_x \Delta f}{2BW} \quad (1) \quad \text{where } N_x \text{ is the size of the readout matrix, } \Delta f \text{ is the chemical shift between water and fat (Hz), and } BW \text{ is the readout bandwidth.}$$

For example, at 1.5T, Δf is -210Hz, and if we choose N_x to be 256, and the bandwidth to be ± 32 kHz, the expected chemical shift is about 0.8 pixels, an acceptable amount of shift. However, at 3.0T, Δf increases to -420Hz, and if we choose N_x to be 512, and the bandwidth to be ± 16 kHz, the expected chemical shift is about 6.7 pixels, a very large shift that will surely degrade image quality. Equation 1 and these examples help illustrate the interplay between field strength, matrix size, and bandwidth and how they affect the expected chemical shift artifact.

In general, N_x is fixed and we choose the lowest possible bandwidth to maximize SNR, while maintaining acceptable chemical shift artifact; the bandwidth for many clinical protocols is chosen in this way. Unfortunately, the chemical shift artifact worsens at higher field strengths. This can be compensated with higher bandwidths, partially offsetting the SNR benefits of the higher field strength.

Fat Suppression

Reliable and uniform fat-suppression is essential for accurate diagnoses in many areas of MR imaging. This is particularly true for sequences like fast spin-echo (FSE), spoiled gradient echo (SPGR), and steady-state free precession (SSFP) imaging where fat is bright and may obscure underlying pathology. Reliable fat-suppression has the added benefit of eliminating chemical shift artifact, by virtue of the fact that fat signal is no longer present, and therefore may allow the use of lower bandwidths that can be used to improve SNR. Several commonly used approaches for fat-suppression are now described.

Spectrally Selective Saturation Pulses: “Fat-Sat”

Spectrally selective saturation (90°) or inversion (180°) pulses are commonly used with many pulse sequences for reliable and effective suppression of fat-signal (2). These pulses rely on the difference in resonant frequency between water and fat, and using RF energy transmitted in a narrow frequency spectrum centered at the fat-peak they are used to destroy the longitudinal magnetization of fat within the object. They are usually followed immediately by a crusher gradient, after which the standard imaging sequence is played. Fat-sat pulses are highly effective in regions where both the main magnetic field (B_0) and the RF field from the coil (B_1) are relatively homogeneous. Typical applications where fat-sat pulses are effective include the knee, pelvis, and abdomen. The primary disadvantages of fat-sat pulses is that they are relatively sensitive to field inhomogeneities that shift the position of the water and fat peaks with respect to the

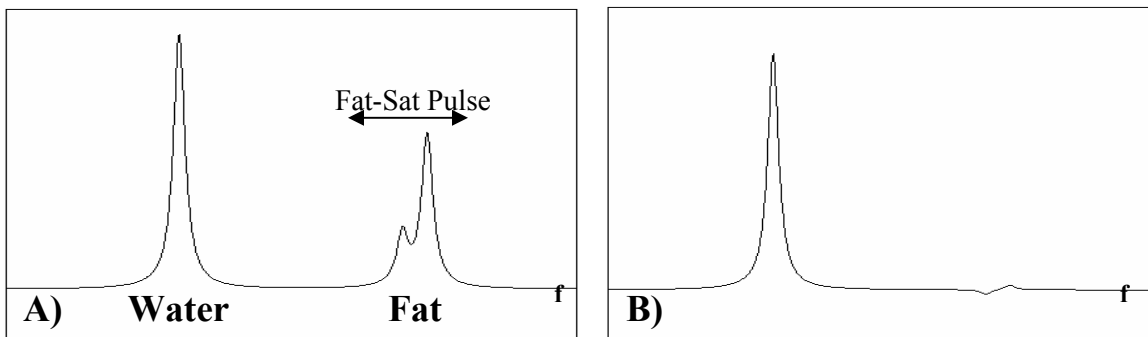


Figure 3: Schematic spectrum of water and fat peaks and the positioning of a spectrally selective saturation (“fat-sat”) pulse over the primary fat peaks, -210Hz from the water peak, before (A) and after (B) the application of the fat-sat pulse.

frequency of the fat-sat pulse. This can result in failed fat suppression, and even cause inadvertent suppression of water signal. Fat-sat pulses are also sensitive to RF inhomogeneities and do not perform well with transmit surface coils; one must rely on coils with uniform RF fields, such as head, body and extremity coils..

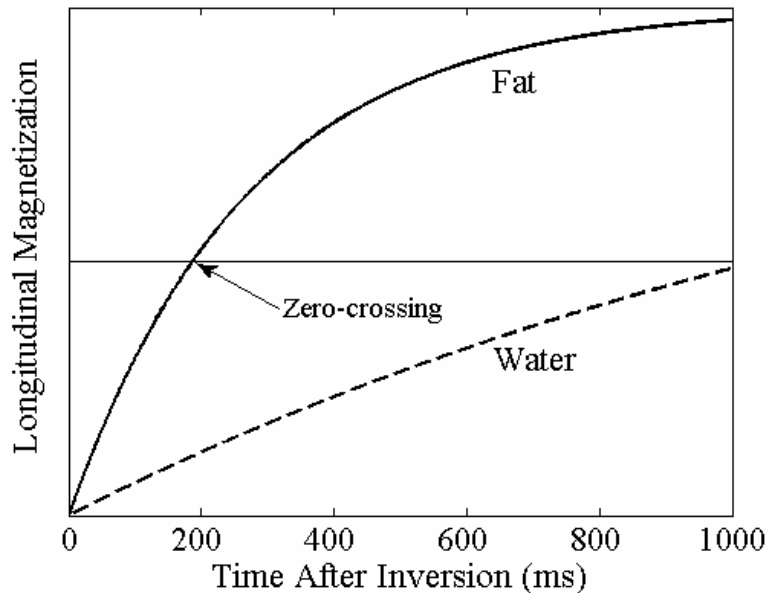
Short Tau Inversion Recovery (“STIR”)

Effective fat-suppression can also be achieved by exploiting T_1 differences between fat and soft tissues containing water. Short tau inversion recovery or “STIR” pulses play a broad spectrum inversion pulse that rotates all magnetization (water and fat) along the $-M_z$ axis (3). Fat has a shorter T_1 than most soft tissues and if an image is acquired as the longitudinal magnetization of fat is crossing through zero (“zero-

crossing”), the signal from fat will be nulled in the resulting image (figure 3). The zero-crossing occurs at approximately 200ms. STIR is a highly reliable method of fat-suppression, and although it is sensitive to RF inhomogeneities, it is very insensitive to field inhomogeneities, which are generally more problematic. STIR can be used a wide variety of challenging applications such as foot/ankle, spine, neck, brachial plexus, orbits, and wrist, etc. An inherent disadvantage of STIR imaging is its inability to perform T1W imaging, particularly after IV contrast, so that STIR is limited to proton density or T2W imaging. In addition the SNR performance is relatively poor and the relatively long

Figure 4: Short-tau inversion recovery imaging acquires images approximately 200ms after the inversion pulse, during the fat zero-crossing, providing robust fat suppression, but poor SNR performance.

inversion time impairs speed performance and sequence efficiency.



Spectral-Spatial Excitation and Water Selective Pulses

A more advanced approach is to exploit differences in resonant frequency between water and fat by direct excitation of the water peak, rather than suppression of the fat peak(4,5). One of the earliest implementations, known as “spectral-spatial” pulses invokes the concept of adding a spectral dimension to excitation k -space (4). The details of this notation are beyond the scope of this abstract, although spectral-spatial pulses can be explained in a simplified manner, as follows. Consider a train of slice-selective “ α ” pulses, each with a small tip angle, α , eg. 5-10°. These α pulses are separated by the time needed for fat to precess 180° relative to water, or $T=1/(2\Delta f)$, about 2.3ms at 1.5T. As shown in figure 4, after the first α pulse, both fat and water are tipped α degrees from the z -axis. Immediately before the next pulse, however, the fat has precessed 180° in the transverse plane, and is subsequently tipped back along the M_z axis, while the water continues its trajectory towards the transverse plane. A more accurate and detailed description of spectral-spatial pulses is found elsewhere (4).

Spectral-spatial pulses are a very effective means of exciting water within an image and are most commonly used in conjunction with spiral imaging and echo planar

imaging (EPI), although it can be combined with other sequences such as spoiled gradient echo and fast spin-echo imaging (6,7). Although spectral-spatial pulses are relatively insensitive to RF inhomogeneities, they remain sensitive to field inhomogeneities, similar to conventional fat-sat pulses (4). Its other major drawback is the need for lengthy pulses, and for this reason spectral pulses are most commonly used with sequences with longer TR's (eg. spiral, EPI).

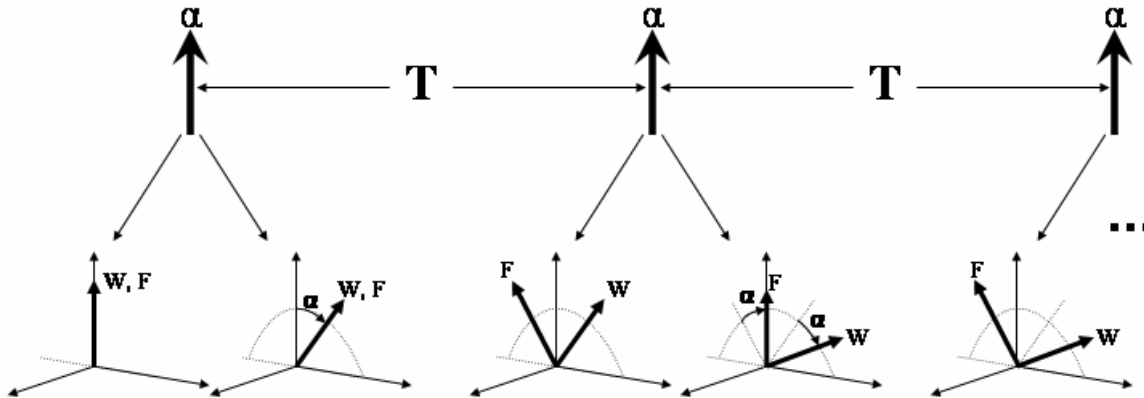


Figure 5: Schematic of spectral-spatial pulses. α pulses are separated by a time, T , sufficient to create a 180° phase shift between water and fat. T is approximately 2.3ms at $1.5T$. Immediately after the first α pulse, water and fat are tipped together, however immediately before the next α pulse, the fat has precessed 180° such that after the second α pulse, the fat is tipped back up along the M_z axis and the water is tipped further towards the transverse plane.

“Dixon” Water-Fat Separation Methods

The final method for fat-suppression discussed in this work is the class of approaches known as “Dixon” water-fat separation (1,8-11). Unlike the methods described above, which suppress fat signal or selectively excite water, Dixon methods rely on the phase shifts created by fat-water resonant frequency differences to *separate* water from fat. In this way, water and fat signals can each be visualized directly. The initial approach proposed by Dixon (8) acquired two images at different TE's such that water and fat were “in-phase” ($S_{in}=W+F$) or “out of phase” ($S_{out}=W-F$). By adding and subtracting S_{in} and S_{out} , water (W) and fat (F) can be separated. The original approach required only two images, but was relatively sensitive to field inhomogeneities, and has been modified to a variety of “three-point” methods that compensate for these inhomogeneities (1,9-11). More recent approaches (11) allow arbitrary and unequally spaced echoes that permit SNR optimization and are helpful for specific applications. All Dixon approaches are insensitive to both RF inhomogeneities and provide robust water-fat separation despite the presence of field inhomogeneities. They are compatible with a wide variety of pulse sequences including T2W-FSE, T1W-FSE, SPGR, and SSFP. Figure 6 is an example of sagittal T1W-FSE images and coronal T2W-FSE images for the cervical spine and brachial plexus of a normal volunteer, comparing fat-saturation with Dixon imaging. Tremendous improvement in the quality of fat-suppression can be seen with the Dixon images. Fat-saturation typically fails in this region of the body because of the unfavorable geometry of the lung apices and neck where large

susceptibility differences create severe magnetic field inhomogeneities. Fat images and recombined images are also available for review with the Dixon method (not shown).

An interesting advantage of Dixon imaging is the ability to recombine water and fat images together, after the fat image has been shifted to correct for chemical shift artifact. This opens interesting possibilities for low-bandwidth imaging and imaging at higher field strengths, *free* from chemical shift artifact. The primary disadvantage of all Dixon methods is the increased scan times required to acquire the images necessary to separate water from fat. Despite this, the decomposition is highly SNR efficient if the correct choice of TE's are used (12). With the correct choice of echoes, the signal from the three images is used with maximum efficiency in the calculation of the water and fat images. Methods for scan time reduction is currently being investigated through partial k-space acquisition methods and parallel imaging (13,14). The latter approach is highly complementary to Dixon imaging, because SNR penalties of parallel imaging are exactly offset by gains in the SNR from the Dixon reconstruction.

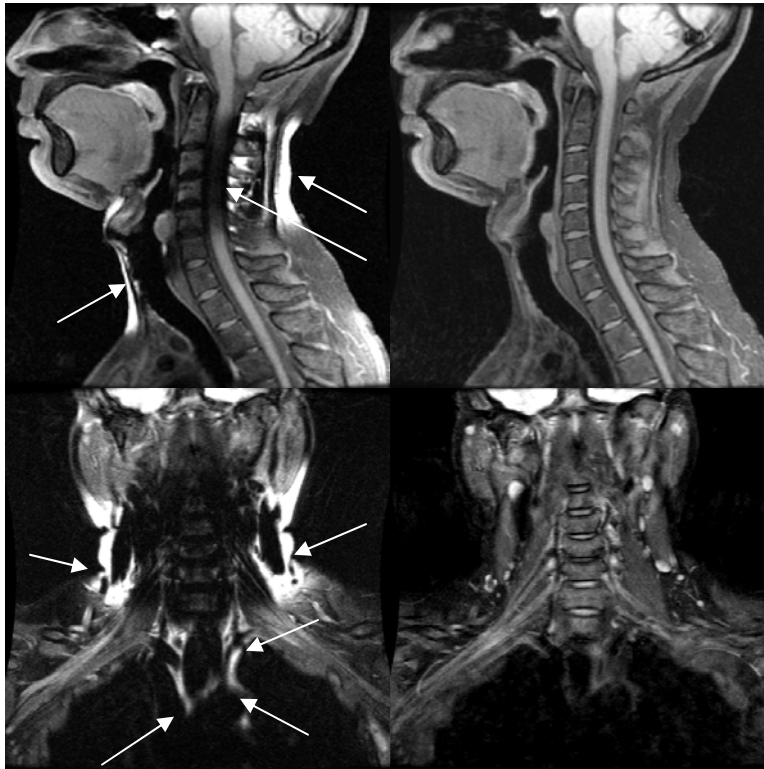


Figure 6: Sagittal T1W-FSE images (top row) and coronal T2W-FSE images (bottom row) of the cervical spine and brachial plexus. Tremendous improvement in fat-suppression quality is seen with Dixon imaging (right column) compared with conventional fat-saturated images (left column). Arrows depict areas of failed fat suppression or inadvertent water suppression.

References:

1. Xiang Q, An L. Water-fat imaging with direct phase encoding. *Journal of Magnetic Resonance Imaging* 1997;7:1002-1015.
2. Keller PJ, Hunter WW, Jr., Schmalbrock P. Multisection fat-water imaging with chemical shift selective presaturation. *Radiology* 1987;164(2):539-541.
3. Bydder GM, Pennock JM, Steiner RE, Khenia S, Payne JA, Young IR. The short TI inversion recovery sequence--an approach to MR imaging of the abdomen. *Magn Reson Imaging* 1985;3(3):251-254.

4. Meyer CH, Pauly JM, Macovski A, Nishimura DG. Simultaneous spatial and spectral selective excitation. *Magn Reson Med* 1990;15(2):287-304.
5. Schick F. Simultaneous highly selective MR water and fat imaging using a simple new type of spectral-spatial excitation. *Magn Reson Med* 1998;40(2):194-202.
6. Leong CS, Daniel BL, Herfkens RJ, Birdwell RL, Jeffrey SS, Ikeda DM, Sawyer-Glover AM, Glover GH. Characterization of breast lesion morphology with delayed 3DSSMT: an adjunct to dynamic breast MRI. *J Magn Reson Imaging* 2000;11(2):87-96.
7. Block W, Pauly J, Kerr A, Nishimura D. Consistent fat suppression with compensated spectral-spatial pulses. *Magn Reson Med* 1997;38(2):198-206.
8. Dixon W. Simple proton spectroscopic imaging. *Radiology* 1984;153:189-194.
9. Glover GH, Schneider E. Three-point Dixon technique for true water/fat decomposition with B₀ inhomogeneity correction. *Magn Reson Med* 1991;18(2):371-383.
10. Ma J, Singh SK, Kumar AJ, Leeds NE, Broemeling LD. Method for efficient fast spin echo Dixon imaging. *Magn Reson Med* 2002;48(6):1021-1027.
11. Reeder SB, Wen Z, Yu H, Pineda AR, Gold GE, Markl M, Pelc NJ. Multicoil Dixon Chemical Species Separation with an Iterative Least-Squares Estimation Method. *Magn Reson Med* 2004;51:35-45.
12. Reeder, SB and Pineda, AR and Wen, Z and Shimakawa, A and Yu, H and Brittain, JH and Gold, GE and Beaulieu, CF and Pelc, NJ, "Iterative "Dixon" Water-Fat Separation with Echo Asymmetry and Least Squares Estimation (IDEAL): Application with Fast Spin-Echo Imaging", 2005 54(3):636-44 *Magn Reson Med*.
13. Sodickson DK, Manning WJ. Simultaneous acquisition of spatial harmonics (SMASH): fast imaging with radiofrequency coil arrays. *Magn Reson Med* 1997;38(4):591-603.
14. Pruessmann KP, Weiger M, Scheidegger MB, Boesiger P. SENSE: sensitivity encoding for fast MRI. *Magn Reson Med* 1999;42(5):952-962.